



# Introducing the Chiral Constrained $\alpha$ -Trifluoromethylalanine in Aib Foldamers to Control, Quantify and Assign the Helical Screw-Sense\*\*

Lizeth Boderó, Karine Guitot, Nathalie Lensén, Olivier Lequin, Thierry Brigaud,  
Sandrine Ongerí, Grégory Chaume

## ► To cite this version:

Lizeth Boderó, Karine Guitot, Nathalie Lensén, Olivier Lequin, Thierry Brigaud, et al.. Introducing the Chiral Constrained  $\alpha$ -Trifluoromethylalanine in Aib Foldamers to Control, Quantify and Assign the Helical Screw-Sense\*\*. Chemistry - A European Journal, 2022, 28 (8), pp.e202103887. <10.1002/chem.202103887>. <hal-03626224>

**HAL Id: hal-03626224**

**<https://hal.science/hal-03626224v1>**

Submitted on 1 Apr 2022

**HAL** is a multi-disciplinary open access archive for the deposit and dissemination of scientific research documents, whether they are published or not. The documents may come from teaching and research institutions in France or abroad, or from public or private research centers.

L'archive ouverte pluridisciplinaire **HAL**, est destinée au dépôt et à la diffusion de documents scientifiques de niveau recherche, publiés ou non, émanant des établissements d'enseignement et de recherche français ou étrangers, des laboratoires publics ou privés.



HAL Authorization

# Introducing the Chiral Constrained $\alpha$ -Trifluoromethylalanine in Aib foldamers to Control, Quantify and Assign the Helical Screw-Sense\*\*

Lizeth Bodero,<sup>[a]</sup> Karine Guitot,<sup>[a]</sup> Nathalie Lensen,<sup>[a]</sup> Olivier Lequin,<sup>[c]</sup> Thierry Brigaud,<sup>[a]</sup> Sandrine Onger, <sup>[b]</sup> Grégory Chaume<sup>\*,[a]</sup>

- [a] Dr. Lizeth Bodero, Dr. Karine Guitot, Dr. Nathalie Lensen, Prof. Thierry Brigaud, Dr. Grégory Chaume  
CY Cergy Paris Université, CNRS, BioCIS  
95000 Cergy Pontoise, France  
E-mail: [gregory.chaume@cyu.fr](mailto:gregory.chaume@cyu.fr)
- [b] Prof. Sandrine Onger  
Université Paris-Saclay, CNRS, BioCIS  
92290 Châtenay-Malabry, France  
E-mail: [sandrine.onger@universite-paris-saclay.fr](mailto:sandrine.onger@universite-paris-saclay.fr)
- [c] Prof. Olivier Lequin  
Sorbonne Université, École Normale Supérieure, PSL University, CNRS, Laboratoire des Biomolécules, LBM  
75005 Paris, France
- [\*\*] Aib= $\alpha$ -aminoisobutyric acid

Supporting information for this article is given via a link at the end of the document.

**Abstract:** Oligomers of  $\alpha$ -aminoisobutyric acid (Aib) are achiral peptides that adopt  $3_{10}$  helical structures with equal population of left- and right-handed conformers. Yet, the screw-sense preference of the helical chain may be controlled by a single chiral residue located at one terminus.  $^1\text{H}$  and  $^{19}\text{F}$  NMR, X-ray crystallography and circular dichroism studies on new Aib oligomers show that the incorporation of a chiral quaternary  $\alpha$ -trifluoromethylalanine at their *N*-terminus induces a reversal of the screw-sense preference of the  $3_{10}$ -helix compared to that of a non-fluorinated analogue having an L- $\alpha$ -methyl valine residue. This work demonstrates that, among the many particular properties of introducing a trifluoromethyl group into foldamers, its stereo-electronic properties are of major interest to control the helical screw sense. Its use as an easy-to-handle  $^{19}\text{F}$  NMR probe to reliably determine both the magnitude of the screw-sense preference and its sign assignment is also of remarkable interest.

## Introduction

Replicating protein folding through synthetic molecules is a main approach in chemical biology. These synthetic analogs called foldamers can be defined as oligomers with a strong tendency to fold into well-defined secondary structures such as helices, sheets or turns, able to mimic the structural properties of proteins.<sup>[1,2]</sup> In particular, the field of peptide-based foldamers has gained considerable interest in medicinal chemistry to circumvent some of the issues of short peptides by increasing their conformational stability and their stability towards proteolysis.<sup>[3,4]</sup> This feature makes peptidomimetic foldamer chemistry an important resource for the design of cell penetrating peptides (CPP),<sup>[5–9]</sup> antimicrobial peptides (AMP)<sup>[10–12]</sup> and inhibitors of protein-protein interactions (PPI).<sup>[13,14]</sup>

Among the different types of foldamers, those constituted by several units of  $\alpha$ -aminoisobutyric acid (Aib) have been widely investigated for their ability to form stable  $3_{10}$ -helices<sup>[15,16]</sup> and their similitude with peptaibols, a natural type of AMP.<sup>[17,18]</sup> Because of the achiral nature of Aib, these hydrophobic foldamers do not exhibit axial chirality and present equal population of left-handed (*M*) and right-handed (*P*) helical screw-senses. Nevertheless, it is possible to alter this equilibrium between the two forms and to induce a screw-sense preference by introducing chiral units, called controllers, at the *C*- or the *N*-terminus. Clayden et al. have shown that the control of the screw-sense preference could be achieved more readily from the *N*- than from the *C*-terminus.<sup>[19]</sup> They also demonstrated that the left- or right-handed sense of helical induction arises from the nature of the  $\beta$ -turn at the *N*-terminus: tertiary amino acids (e.g. L-Val) induce left-handed helicity through a type II  $\beta$ -turn while quaternary amino acids (e.g. L- $\alpha$ -methylvaline) favor right-handed helicity via a type III  $\beta$ -turn.<sup>[20,21]</sup> The screw-sense preference can be quantified using different  $^1\text{H}$ ,  $^{19}\text{F}$  and  $^{13}\text{C}$  NMR spectroscopic probes along with CD, IR spectroscopy and X-ray crystallography.<sup>[22,23]</sup>

The use of fluorine-containing amino acids is becoming a very promising tool for the design of new bioactive molecules.<sup>[24,25]</sup> However, their use for the design of fluorinated peptide-based foldamers remains in its infancy with only a few examples reported so far.<sup>[26–31]</sup>

We aim to give some inputs in the vast but unknown field of exploring the rational incorporation of fluorine atoms into peptidomimetic foldamers to lead to novel molecular architectures, and to improve or modulate their physicochemical properties, and their biological profile. As  $\alpha$ -trifluoromethyl- $\alpha$ -amino acids (Tfm-AAAs) are interesting to promote the helical secondary structures of peptides,<sup>[31–33]</sup> we propose here to investigate the ability of (*R*)- and (*S*)- $\alpha$ -trifluoromethylalanine (TfmAla) to stabilize the  $3_{10}$

## RESEARCH ARTICLE

helical conformation and to induce a screw-sense preference when incorporated at the *N*-terminus of short Aib oligomers. Because of the stereo-electronic effects of the trifluoromethyl group (CF<sub>3</sub>), additional advantages are also expected for the fluorinated oligomers compared to their non-fluorinated analogs, including hydrophobicity, thermal resistance, conformational constraint, polarization effects on neighboring groups as well as H-bonding and dipole induction.<sup>[34-41]</sup> The CF<sub>3</sub> group can also be used as a highly sensitive probe for <sup>19</sup>F NMR spectroscopy.<sup>[32,33,42]</sup> In contrast with achiral <sup>19</sup>F NMR reporters based on β,β'-difluoroAib inserted at the *C*-terminus,<sup>[43]</sup> TfmAla has been investigated here as a multiple tool: first, as a chiral controller to induce a screw-sense preference, and second, as an NMR reporter to both quantify and assign it. It could also contribute to provide other valuable information about the fluorinated foldamers (orientation in membrane, conformation, dynamics, interactions with partners, kinetics of degradation, ...).<sup>[42]</sup>

## Results and Discussion

Two series of fluorinated Aib foldamers have been designed (Figure 1). The first series is based on the incorporation of a single fluorinated chiral residue, namely (*S*)- or (*R*)-Cbz-TfmAla, at the *N*-terminal position of Aib pentamers, constituting a sufficient length to ensure the stabilization of the 3<sub>10</sub> helical conformation.<sup>[20,21,44-46]</sup> The introduction of *C*-terminal ester groups can locally disturb the regular helical structure of peptide derivatives, and this effect is known as *C*-terminal destabilising Schellman motif. Since the size of the *C*-terminal ester group and the resulting Schellman motif can play a significant role in determining the overall secondary structure of short Aib sequences in solution,<sup>[47]</sup> we prepared two sets of compounds bearing respectively a methyl (OMe) (**1**) and a *tert*-butyl (OtBu) (**2**) ester. In the second series, a glycine residue was added at the *C*-terminal position to quantify the induced screw-sense preference of the helix. Indeed, compared to other NMR reporters,<sup>[20]</sup> the glycine at the *C*-terminus has been reported to be more suitable, not only because of its availability and its easy incorporation into peptides, but above all because the signals of its pair of diastereotopic protons stand clear of the other resonances in the <sup>1</sup>H NMR spectrum, allowing the ready observation of their anisochronicity (chemical shift separation). Two different protecting groups, namely Cbz (compounds **3**) and

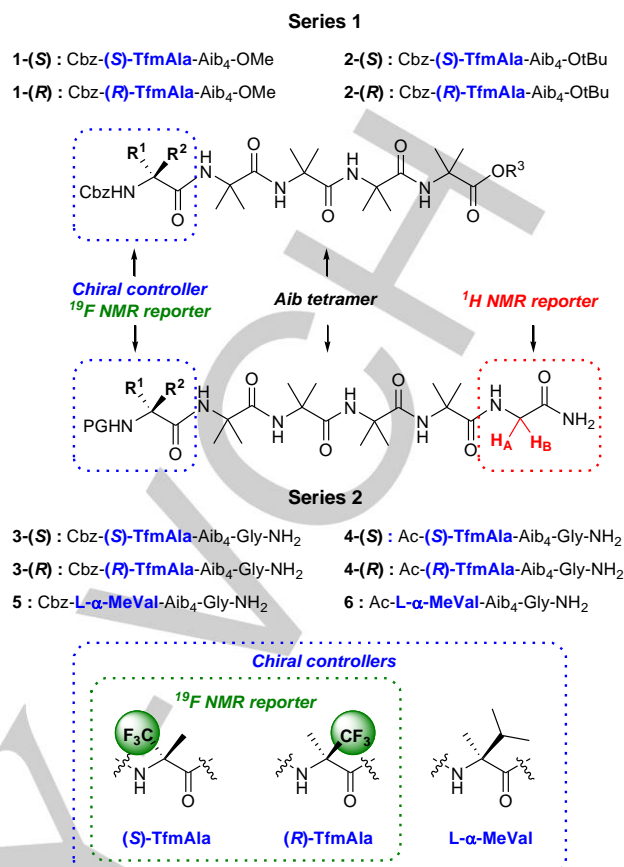
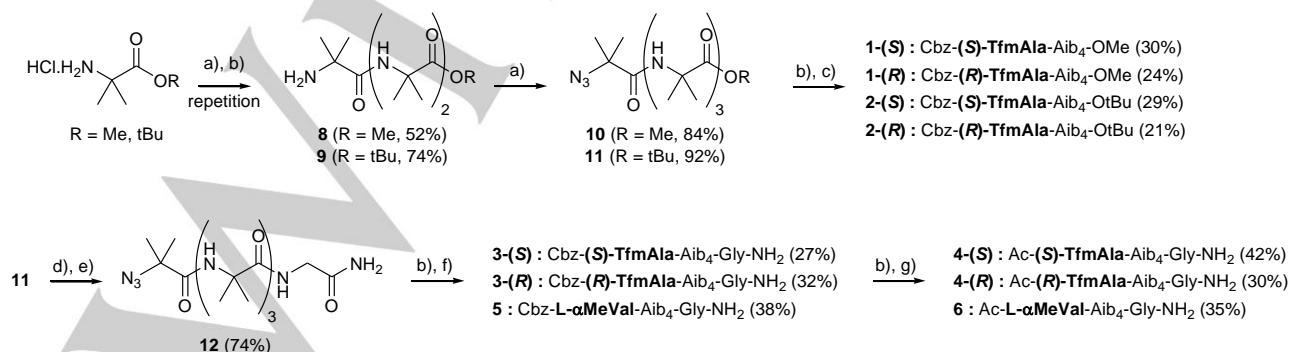


**Figure 1.** Chemical structure of the target fluorinated foldamers **1-4** and non-fluorinated analogues **5-6** (Ref 44-46).

acetyl (Ac) (compounds **4**), were introduced at the *N*-terminus to assess their effect on the level of control of the chiral controller even if it has been reported that, in general, the control by quaternary amino acid is maximized by a carbamate protecting group.<sup>[19]</sup> Reference compounds **5** and **6**, containing the L-α-methylvaline residue (L-α-MeVal) as chiral controller and previously reported by Clayden's group,<sup>[20,21,44]</sup> were also prepared to study the conformations obtained with fluorinated oligomers compared to non-fluorinated ones. The helical conformation and screw-sense preference of the synthesized oligomers were studied using CD spectroscopy, X-ray crystallography, and different NMR probes, including the



**Scheme 1.** Synthesis of foldamers **1-6**: a) N<sub>3</sub>-Aib-Cl **7**, Et<sub>3</sub>N, DCM, 0 °C to rt, overnight; b) H<sub>2</sub> (1 bar), Pd/C (10% w/w), MeOH, rt, overnight; c) Cbz-(*S*)-Tfm-Ala or Cbz-(*R*)-Tfm-Ala, EDC.HCl, HOBT, *i*Pr<sub>2</sub>NEt, DMF, 0 °C to rt, overnight; d) TFA/DCM 1:1, overnight; e) Ac<sub>2</sub>O, HCl.GlyNH<sub>2</sub>, *i*Pr<sub>2</sub>NEt, reflux 72 h; f) Cbz-(*S*)-Tfm-Ala, Cbz-(*R*)-Tfm-Ala or Cbz-L-α-MeVal, EDC.HCl, HOBT, *i*Pr<sub>2</sub>NEt, DMF, 0 °C to rt, overnight; g) Ac<sub>2</sub>O, *i*Pr<sub>2</sub>NEt, DCM, rt, overnight.

## RESEARCH ARTICLE

measurement of anisochronicity between the C-terminal diastereotopic “reporter” protons and  $^{19}\text{F}$  NMR spectroscopy. Oligomers **1–6** were synthesized as indicated in Scheme 1. Aib tetramers precursors **10** and **11** bearing respectively a methyl or a *tert*-butyl ester at the C-terminus were prepared following the reported procedure via iterative coupling of  $\text{N}_3\text{-Aib-Cl}$  **7** and reduction of the *N*-terminal azide functional group.<sup>[45–47]</sup> The pentamer **12**<sup>[44]</sup> containing a C-terminal glycnamide residue was obtained upon removal of the *tert*-butyl group of **11**, activation with acetic anhydride and reaction with glycnamide hydrochloride. The incorporation of the Cbz-protected quaternary amino acids (*S*)- and (*R*)-TfmAla<sup>[48,49]</sup> and L- $\alpha$ -MeVal at the *N*-terminal position was carried out after the azide reduction of **10**, **11** and **12** under typical EDC/HOBt coupling conditions in solution to afford the final compounds **1–3** and **5**.<sup>[21]</sup> The Cbz group of **3** and **5** was also substituted by an acetyl by catalytic hydrogenolysis and further treatment with acetic anhydride to provide the peptides **4** and **6**.<sup>[21]</sup> The screw-sense preference of the fluorinated foldamers **1–4** was determined and compared with the non-fluorinated ones **5** and **6**, by acquiring their CD spectra in methanol. This solvent is trickier for preserving intramolecular hydrogen bonding and folding in comparison with aprotic organic solvents but it was chosen for comparison with data reported in the literature for Aib oligomers and as the closest solvent to water.

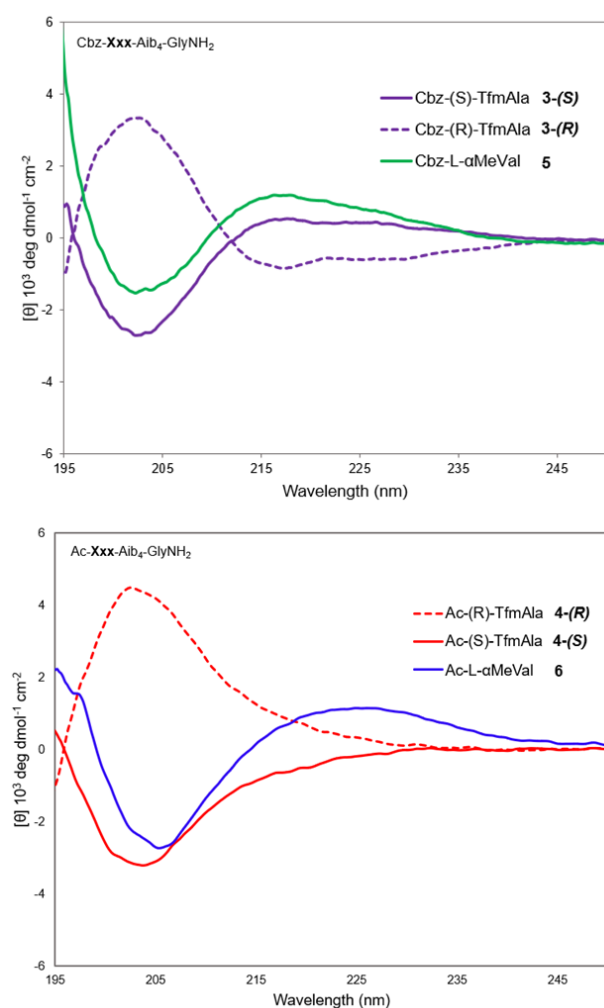


**Figure 2.** CD spectra of peptides **3–6** (0.3 mM in MeOH, 20°C)

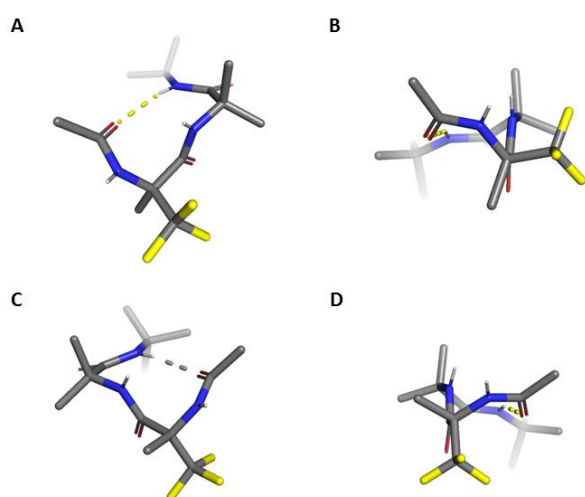
In Figure 2 are shown the CD spectra of the compounds **3–6** of the series **2** (see Supporting Information Figures S1 and S2 for the CD spectra of **1** and **2** respectively). The fluorinated compounds **1–4**, regardless of the identity of the *N*-terminal protecting group, exhibited a major band near 205 nm, which plays a central role in the assignment of  $3_{10}$  helix handedness, as proven by experimental and DFT-calculated CD spectra.<sup>[44]</sup> A weaker band near 220 nm has previously been observed as a shoulder of the main band. This is apparent in the spectra of **3** but not compound **4**. These features are similar to the spectra of the reference compounds **5–6** and consistent with a  $3_{10}$ -helix structure.<sup>[50]</sup> Moreover, the CD spectra of the *R* enantiomers of the fluorinated foldamers **1–4** resulted in the mirror image of the corresponding *S* peptides, indicating the opposite screw-sense orientation of the  $3_{10}$ -helices. In agreement with the literature, the negative band at 205 nm indicated that the *N*-terminal quaternary L- $\alpha$ -MeVal of the reference compounds **5** and **6** induces a right-handed helicity (*P*).<sup>[44,50]</sup> Surprisingly, the Cbz-protected compound **3-(S)** and its *N*-acetylated analogue **4-(S)** exhibited similar CD signature to the ones of the reference compounds **5** and **6**, respectively. This result was unexpected as the van der Waals volume of the  $\text{CF}_3$  group is reported to be only slightly larger than that of the isopropyl group (*i*-Pr),<sup>[51]</sup> which would make peptides **3-(R)** and **4-(R)** the isosteric analogues of the reference compounds **5** and **6**, respectively. Therefore, the reversal of the screw-sense orientation observed for the fluorinated foldamers may be rather attributed to the electronic effects conferred by the  $\text{CF}_3$  group.

Recrystallization of peptide **4-(S)** from MeOH/H<sub>2</sub>O gave crystals suitable for solid state structure analysis by X-ray crystallography (CCDC reference numbers: 2107837 (**4-(S)**)). However, this could not be used to confirm the preferential helical screw-sense observed in solution by CD. Indeed, the crystallographic structure of **4-(S)** showed two independent conformers **4-(S)<sub>M</sub>** and **4-(S)<sub>P</sub>** with opposite screw-sense, aligned in an antiparallel arrangement in the asymmetric cell unit and held together through (C-terminal acetamido)  $\text{N-H}\cdots\text{C=O}$  (Aib<sup>4</sup> residue) intermolecular hydrogen bonds (1.99 Å and 2.06 Å) (see Supporting Information Figure S3). This result suggests that the crystallization favors the selection of the two screw-sense helices in the cell unit. Similar observations have been reported on related Aib compounds showing structures in the crystal state different to the conformational preference observed in solution.<sup>[21,52,53]</sup> The structures of each conformer of **4-(S)** in the solid state indicate the presence of five consecutive  $i + 3 \rightarrow i$   $\text{N-H}\cdots\text{C=O}$  bonds, consistent with the  $3_{10}$  helical conformation (Table 1 and Figure S4 in Supporting Information). Inspection of the  $\phi$ ,  $\psi$  backbone torsion angles in Table 1 reveals that the two conformers (**4-(S)<sub>M</sub>** and **4-(S)<sub>P</sub>**) form mainly  $3_{10}$ -helical structures along their Aib<sub>4</sub> peptide chain. These angles exhibit similar values but opposite signs, indicating reversed screw-senses in the two structures. For the conformer **4-(S)<sub>M</sub>**, the  $\phi$ ,  $\psi$  torsion angle values of Aib residues range from 54.3° to 57.4° and 26.4° to 32.6°, respectively, close to those typical for left-handed (*M*)  $3_{10}$ -helix (57°, 30°) while for **4-(S)<sub>P</sub>**, the  $\phi$ ,  $\psi$  values range from –53.8° to –59.5° and –27.4° to –33.0°, respectively, close to those typical for right-handed (*P*)  $3_{10}$ -helix (–57°, –30°).<sup>[53]</sup> Due to the presence of the Gly-NH<sub>2</sub> residue, the  $3_{10}$  helix conformation of **4-(S)<sub>M</sub>** and **4-(S)<sub>P</sub>** is slightly distorted at the C-terminus with the presence of a type I/I'  $\beta$ -turn ( $\phi = -90^\circ$ ,  $\psi = 0^\circ$  and  $\phi = 90^\circ$ ,  $\psi = 0^\circ$ , respectively). The helical screw-sense of the two structures



**Table 1.** Structural parameters for conformers **4-(S)<sub>M</sub>** and **4-(S)<sub>P</sub>** observed in the X-ray structure of **4-(S)**

Residue	<b>4-(S)<sub>M</sub></b>			<b>4-(S)<sub>P</sub></b>		
	$\phi$ (deg)	$\psi$ (deg)	$i - 1$ (C=O) to $i + 2$ (H-N) H-bonding distance (Å)	$\phi$ (deg)	$\psi$ (deg)	$i - 1$ (C=O) to $i + 2$ (H-N) H-bonding distance (Å)
(S)-TfmAla <sup>1</sup>	47.3	42.3	2.11	-32.1	-57.9	2.03
Aib <sup>2</sup>	55.8	32.6	2.27	-59.5	-31.4	2.28
Aib <sup>3</sup>	57.4	26.8	2.13	-57.0	-27.4	2.15
Aib <sup>4</sup>	54.9	26.4	2.06	-54.4	-28.6	2.05
Aib <sup>5</sup>	54.3	31.4	2.17	-53.8	-33.0	2.10
Gly <sup>6</sup>	81.8	10.2		-80.8	-9.6	

**Figure 3.** First turn conformation as observed in the X-ray crystal structure of peptide **4-(S)** (the rest of the molecule is omitted for clarity). **A:** side view of conformer **4-(S)<sub>M</sub>**; **B:** top view of conformer **4-(S)<sub>M</sub>**; **C:** side view of conformer **4-(S)<sub>P</sub>**; **D:** top view of conformer **4-(S)<sub>P</sub>**. Conformers **4-(S)<sub>M</sub>** and **4-(S)<sub>P</sub>** display left-handed (*M*) and right-handed (*P*)  $3_{10}$  helical conformation, respectively. Intramolecular H-bonds are indicated as dashed.

seems to be driven by the  $\phi$ ,  $\psi$  backbone torsion angles of the chiral TfmAla residue at the *N*-terminal position. Because quaternary L- $\alpha$ -MeVal residue is reported to favor right-handed helicity via a type III  $\beta$ -turn,<sup>[20]</sup> it was anticipated that the (S)-TfmAla, a fluorinated analogue of the D- $\alpha$ -MeVal, would also promote left-handed helicity. However, this was opposite to the experimental CD results, that showed a major right-handed helix conformation. In the **4-(S)<sub>M</sub>** conformer, the TfmAla<sup>1</sup> displays positive torsion angles ( $\phi = 47.3^\circ$ ,  $\psi = 42.3^\circ$ ) corresponding to a slightly distorted type III'  $\beta$ -turn ( $\phi = 60^\circ$ ,  $\psi = 30^\circ$ ), but allowing a left-handed helicity (Figure 3A). The CF<sub>3</sub> group of the TfmAla, corresponding to the bulkiest group, is almost perpendicular to the C=O group (the torsion angle of F<sub>3</sub>C-C $\alpha$ -C=O is 103.3°) (Figure 3B). In contrast, the TfmAla<sup>1</sup> of the **4-(S)<sub>P</sub>** conformer displays negative torsion angles ( $\phi = -32.1^\circ$ ,  $\psi = -57.9^\circ$ ) which

significantly deviate from those expected for a type III  $\beta$ -turn, but still allowing the right-handed  $3_{10}$ -helical structure (Figure 3C). Interestingly, these unusual  $\phi$ ,  $\psi$  backbone torsion angles place the CF<sub>3</sub> group eclipsed to the C=O group (the torsion angle of F<sub>3</sub>C-C $\alpha$ -C=O is 6.5°) leading to an alignment of their dipole (Figure 3D). This particular electronic effect of the CF<sub>3</sub> group could thus induce the major right-handed helix conformation of **4-(S)<sub>P</sub>** observed in solution, as indicated by CD experiments.

The fluorinated oligomers **1-4** were then fully characterized by NMR in methanol-*d*<sub>3</sub>, using 2D experiments (e.g., HSQC, HMBC, ROESY) to assign the chemical shifts of <sup>1</sup>H and <sup>13</sup>C NMR resonances. No concentration-dependence was observed in methanol indicating the absence of aggregation. The NMR data of the non-fluorinated oligomers **5** and **6** were in full agreement with those reported in the literature.<sup>[20,44]</sup>

In order to gain insight into the intramolecular H-bond arrangement, the temperature coefficients ( $\Delta\delta/\Delta T$ ) of NH chemical shifts of fluorinated oligomers **1-4** were calculated. In all the compounds, the  $\Delta\delta/\Delta T$  values obtained for NH protons of the Aib residues 3, 4 and 5 were superior to -4 ppb/K, indicating the existence of intramolecular H-bonds (Figure 4), while the two *N*-terminal NH protons exhibit significantly larger temperature coefficients (Tables S6 and S7 in Supporting Information).<sup>[54]</sup> For compounds **3** and **4**, two additional H-bonds were identified involving the NH of the Gly residue and one of the C-terminal amide protons (Figure 4). These results are consistent with the  $i \leftarrow i + 3$  hydrogen bonding pattern of  $3_{10}$  helix structure.<sup>[20]</sup> Conversely to the reported observations on tetrameric Aib oligomers, the presence of the Schellman motif at the C-terminus of oligomers **1** and **2** did not perturb the intramolecular hydrogen-bonding contacts, even when using the more sterically

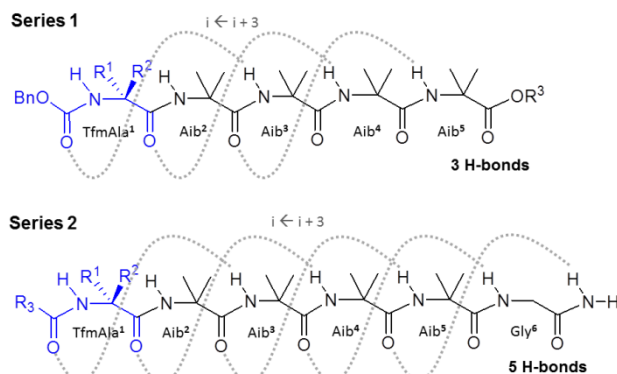


**Figure 4.** H-bond patterns for foldamers **1–4** consistent with  $3_{10}$  helix structures

demanding *tert*-butyl ester.<sup>[47]</sup> We were also pleased to observe that the incorporation of the TfmAla residue at the *N*-terminus of Aib oligomers did not hamper the H-bonding pattern of the  $3_{10}$  helix despite the stronger H-bond donating effect of its vicinal N-H amide due to the electron withdrawing effects of the  $\text{CF}_3$  group. Information from the ROESY spectra of **1–4** in methanol- $d_3$  supports the existence of stable helical conformations. Sequential  $\text{NH}(i)/\text{NH}(i+1)$  ROE correlations, characteristic of  $\alpha$  and  $3_{10}$  helices,<sup>[47,55,56]</sup> were detected in the amide region for all the fluorinated foldamers with no difference within each pair of enantiomers (see Supporting Information Figures S5–S11). Due to signal overlapping, we could not identify any  $\text{CH}_3^{\beta}(i)/\text{NH}(i+2)$  cross-peaks in the ROESY spectra. However, the absence of  $\text{NH}(i)/\text{NH}(i+2)$  cross-peaks supports the  $3_{10}$  helix conformation.<sup>[55]</sup> As a representative example, the ROESY spectrum of compound **4-(S)** is shown in Figure 5.

Further evidence of the helicity of the fluorinated foldamers was given by the anisochronicity of Aib *gem*-dimethyl groups signals in  $^{13}\text{C}$  NMR (see Supporting Information Table S9). This anisochronicity, also known as chemical nonequivalence (CNE), can exceed 2 ppm in the presence of a stable helical conformation.<sup>[20,57]</sup> The CNE values of Aib methyl groups of peptides **1** and **2** were above 2 ppm, with exception of the last Aib residue. This suggests a loss of helicity at C-termini possibly due to the presence of the ester group that has been reported by Clayden *et al.* as destabilizing Schellman motif.<sup>[47]</sup> In the case of peptides **3–6**, containing an additional Gly unit at C-terminus, the CNE values were around 2 ppm for all Aib residues. The slight decrease of the CNE values observed in the *N*-acetyl compounds **4** and **6** compared to their Cbz-analogues **3** and **5** confirms the superior effect of the carbamate protecting group over the acetyl one in stabilizing helical conformation in Aib oligomers.<sup>[19]</sup> Interestingly, a more defined separation pattern was observed for fluorinated peptides **3** and **4** compared to reference compounds **5** and **6**, respectively.

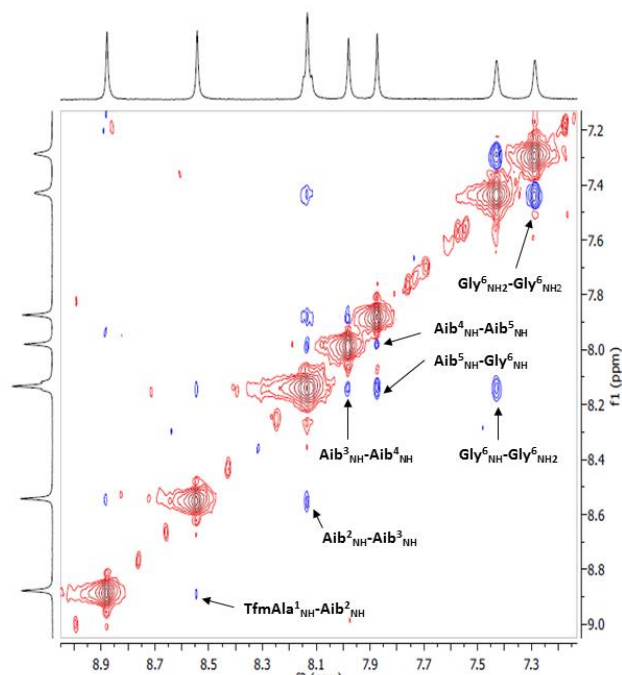


**Figure 5.** Amide region of the ROESY spectrum of compound **4-(S)** (400 MHz,  $\tau_m = 280$  ms, 2.5 mM in  $\text{MeOH}-d_3$ , 298 K).

**Table 2.** Distances (Å) obtained by 2D-NMR and X-ray crystallography for **4-(S)**

Distances	2D-NMR [a]	X-ray of Conformer <b>4-(S)<sub>M</sub></b>	X-ray of Conformer <b>4-(S)<sub>P</sub></b>
TfmAla <sup>1</sup> HN - Aib <sup>2</sup> HN	$3.0 \pm 0.2$	2.92	3.07
Aib <sup>2</sup> HN - Aib <sup>3</sup> HN	$2.7 \pm 0.3$	2.79	2.75
Aib <sup>3</sup> HN - Aib <sup>4</sup> HN	$3.0 \pm 0.3$	2.69	2.63
Aib <sup>4</sup> HN - Aib <sup>5</sup> HN	$3.3 \pm 0.3$	2.83	2.63
Aib <sup>5</sup> HN - Gly <sup>6</sup> HN	$2.6 \pm 0.2$	2.69	2.67
Gly <sup>6</sup> HN - CONH <sub>2</sub>	$2.6 \pm 0.3$	2.55	2.66

[a] NMR-derived distances with their standard deviations

The interproton distances  $\text{NH}(i)/\text{NH}(i+1)$  of **4-(S)** have been estimated from the integration of their cross-peaks observed on the ROESY spectra (See Supporting Information Table S8)<sup>[20]</sup> and compared to the values determined from the X-ray crystal structures **4-(S)<sub>M</sub>** and **4-(S)<sub>P</sub>** (Table 2). There is a good correlation between the three sets of distances and the values, ranging from 2.55 to 3.07 Å, are consistent with the presence of a regular helical conformation both in solution and solid state.

The quantification of the magnitude of the screw-sense preference in solution for compounds **3–6** was then enabled by their NMR spectroscopic probes. First, the helical excess (h.e.) was calculated by measuring the ratio of anisochronicity of the Gly diastereotopic protons at fast and slow exchange regime in methanol (h.e. =  $\Delta\delta_{\text{fast}}/\Delta\delta_{\text{slow}}$ ) (Table 3).<sup>[21,22]</sup> The sign of the helical excess indicated in Table 3 was assigned on the basis of the CD signature (negative in a left-handed helix and positive in a right-handed helix).<sup>[20,21]</sup> The h.e. values for the reference compounds **5** and **6** were first assessed. Compared to those

## RESEARCH ARTICLE

**Table 3.** Anisochronicity in the CH<sub>2</sub> protons of Gly residue

Compound	$\Delta\delta_{\text{fast}}^{293\text{K}}$ (ppb) <sup>[a]</sup>	$\Delta\delta_{\text{slow}}^{193\text{K}}$ (ppb) <sup>[b]</sup>	<sup>1</sup> H NMR reporter h.e. obs <sup>[c]</sup> , h.e. o <sup>[d]</sup> (%)	<sup>19</sup> F NMR reporter h.e. obs <sup>[e]</sup> (%)
<b>3-(S)</b>	261	417	+62, +81	+80
<b>3-(R)</b>	264	419	−63, −83	−80
<b>5</b>	275	382	+72, +95 (+52, +68) <sup>[f]</sup>	
<b>4-(S)</b>	198	417	+47, +62	+66
<b>4-(R)</b>	198	417	−47, −62	−68
<b>6</b>	216	377	+57, +75 (+41, +54) <sup>[f]</sup>	

[a] Chemical shift separation between the anisochronous peaks arising from the diastereotopic protons of the Gly<sup>6</sup> residue in the <sup>1</sup>H NMR spectrum in CD<sub>3</sub>OD at 293 K. [b] Chemical shift separation between the anisochronous peaks arising from the diastereotopic protons of the Gly<sup>6</sup> residue in the <sup>1</sup>H NMR spectrum in CD<sub>3</sub>OD at 193 K. [c] Observed helical excess (h.e. obs) is calculated using h.e. =  $\Delta\delta_{\text{fast}}/\Delta\delta_{\text{slow}}$ , as defined in ref 58. [d] Inferred helical excess (h.e. o) corresponds to the helical excess induced by the controller at the *N*-terminus of the oligomer; see the text for discussion and ref 21. [e] Observed helical excess (h.e. obs) is calculated by integrating the isolated CF<sub>3</sub> resonances in the <sup>19</sup>F NMR spectrum in CD<sub>3</sub>OD at 213 K. [f] In parentheses, h.e. values reported in ref 21. Helical excess (h.e.) is negative in a left-handed helix and positive in a right-handed helix.

reported in the literature,<sup>[21]</sup> peptides **5** and **6** displayed much higher h.e. values (ca. 18% increase). This trend can be ascribed to the fact that the h.e. values from the literature have been calculated from the hypothesized  $\Delta\delta_{\text{slow}}$  value of the GlyNH<sub>2</sub> reporter of ca. 530 ppb.<sup>[21]</sup> In the course of our study, this value was determined experimentally by NMR at very low temperature (−80°C) to ensure the slow exchange regime. The maximum peak separation of the GlyNH<sub>2</sub> reporter measured for peptides **5** and **6** was found to be significantly smaller (ca. 380 ppb), explaining the higher values of their helical excess. The fluorinated peptides **3** and **4** displayed slightly higher  $\Delta\delta_{\text{slow}}$  value (ca. 417 ppb) compared to their non-fluorinated analogues. Their helical excess was similar for each pair of enantiomers and slightly inferior (ca. 10% less) to the reference compounds **5** and **6**, respectively. Moreover, the screw-sense preference of the fluorinated Aib oligomers was more pronounced (ca. 15% higher) in the case of Cbz-protected compounds compared to their *N*-acetylated analogues, as observed in the non-fluorinated series.

Because the CF<sub>3</sub> group can also be used as highly sensitive probe for <sup>19</sup>F NMR spectroscopy, we next investigated the opportunity to use the CF<sub>3</sub> group of the chiral (S)- and (R)-TfmAla residue and <sup>19</sup>F NMR spectroscopy to quantify the magnitude of the screw-sense preference. The presence of this second NMR reporter at the *N*-terminus should allow assessing the degree of control exerted by the chiral TfmAla controller itself and the variation of conformational preference along the peptide chain. <sup>19</sup>F NMR of peptides **3** and **4** at room temperature revealed a single average peak, indicating a fast regime exchange and preventing the quantification of the screw-sense preference (Figure 6 and Figure S13 in Supporting Information). Upon cooling to −60°C, the slow regime exchange was reached and two distinct peaks corresponding to the CF<sub>3</sub> resonances of the (*M*)- and (*P*)-helices were observed. The helical excess of peptides **3** and **4**, obtained by integrating the isolated resonances, were found to be ca. 80% and 67%, respectively (Figure 6 and Figure S13 in Supporting Information). Compared to the helical excess (h.e. obs) measured

at the C-terminus using the Gly-NH<sub>2</sub> <sup>1</sup>H NMR reporter (Table 3), the values observed at the *N*-terminus of peptides **3** and **4** were much higher. This

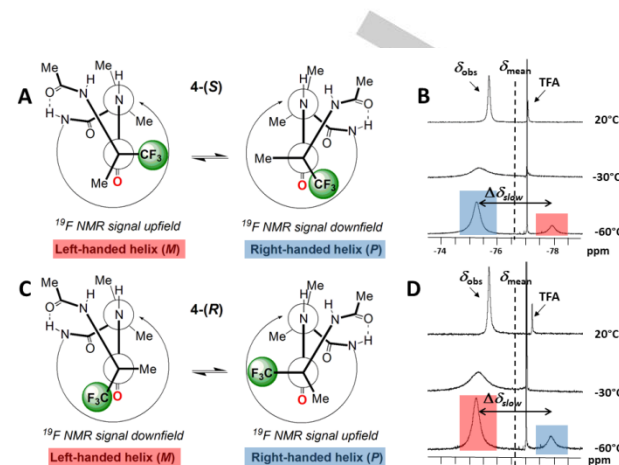


**Figure 6.** A: Newman projections of the *N*-terminal turn of **4-(S)** in left-handed and right-handed helices; B: <sup>19</sup>F NMR spectra of **4-(S)** in CD<sub>3</sub>OD at three different temperatures; C: Newman projections of the *N*-terminal turn of **4-(R)** in left-handed and right-handed helices; D: <sup>19</sup>F NMR spectra of **4-(R)** in CD<sub>3</sub>OD at three different temperatures. <sup>19</sup>F NMR spectra were calibrated by setting the C<sub>6</sub>F<sub>6</sub> peak to −165.37 ppm. The dash line indicates the mean of the chemical shifts at slow regime exchange ( $\delta_{\text{mean}}$ ). TFA: trifluoroacetic acid.

result was anticipated due to the decay of the helical excess along the peptide chain.<sup>[21]</sup> However, it is possible to estimate the control exerted by the chiral controller at the *N*-terminus by extrapolating the measured helical excess (h.e. obs) at the C-terminus using the <sup>1</sup>H NMR reporter (see Supporting Information). The corresponding inferred helical excess values (h.e. o) exerted by peptides **3** and **4** are very similar to those obtained using the <sup>19</sup>F NMR reporter (Table 3).

We next explored the possibility to assign the sign of the screw-sense preference by observing whether the predominant CF<sub>3</sub> signal appears upfield or downfield to that of the minor one. Indeed, the CF<sub>3</sub> group of the chiral TfmAla residue has not the same chiral environment along a right- or a left-handed <sub>310</sub> helix.<sup>[59–61]</sup> Thanks to the CD spectra of peptide **4** (Figure 2), we were able to assign the right-handed (*P*) helix to the downfield major <sup>19</sup>F NMR signal of peptides **4-(S)** (Figure 6B) and the left-handed (*M*) helix to the downfield major <sup>19</sup>F NMR signal of peptides **4-(R)** (Figure 6D). The same observation was done with peptide **3** (see Supporting Information Figure S13). A deep examination of the crystal structure of **4-(S)** gives an explanation for the position of the predominant CF<sub>3</sub> signal relative to the minor signal observed in <sup>19</sup>F NMR spectra. In the structure of **4-(S)<sub>M</sub>**, corresponding to a left-handed <sub>310</sub> helix (*M*), the CF<sub>3</sub> group is staggered with respect to the TfmAla carbonyl group (Figure 3B and 6A) while it is eclipsed with respect to the TfmAla carbonyl group in the right-handed <sub>310</sub> helix (*P*) of the structure of **4-(S)<sub>P</sub>** (Figure 3D and 6A). Therefore, the eclipsed CF<sub>3</sub> group with respect to the TfmAla carbonyl group undergoes a downfield shift in <sup>19</sup>F NMR spectra. This trend is important to note because, in the case of non-fluorinated residues, the more eclipsed alkyl group with respect to the carbonyl was reported as resonating at higher fields (upfield shift) in <sup>13</sup>C NMR spectra.<sup>[44,45,61–64]</sup> The different behavior between the two nuclei with respect to the carbonyl group can be explained by an electric field effect. Indeed, in non-fluorinated series, it has been proposed that the high electron density of the carbonyl oxygen polarizes the C–H bond



## RESEARCH ARTICLE

of the eclipsed methyl group.<sup>[65]</sup> As a result, the carbon atom gains some electron density, causing an upfield shift, while the hydrogen atom undergoes reduced electron density, causing its downfield shift. A similar behavior could be envisioned for the C–F bond of the eclipsed CF<sub>3</sub> group. Thus, this <sup>19</sup>F-NMR parameter can successfully be exploited to assess the helical screw-sense preference of fluorinated Aib-foldamers, provided that the absolute configuration of the Tfm-Ala residue is known. For Aib oligomers with (S)-Tfm-Ala residue at the N-terminus, the CF<sub>3</sub> group of the right-handed (P) helix falls downfield with respect to the CF<sub>3</sub> group of the left-handed (M) helix (Aib oligomers with (R)-Tfm-Ala residue display opposite behavior).

The helical excess (h.e.) of the peptides **3** and **4** can be also estimated by using the relationship:  $\text{h.e.(\%)} = (\delta_{\text{obs}} - \delta_{\text{mean}}) / (\Delta\delta_{\text{slow}} / 2)$ , where  $\delta_{\text{obs}}$  is the chemical shift of the coalesced <sup>19</sup>F NMR signal observed at room temperature (fast exchange regime),  $\delta_{\text{mean}}$  corresponds to the mean of the chemical shift values of the two CF<sub>3</sub> resonances at slow regime exchange, and  $\Delta\delta_{\text{slow}}$  the chemical shift difference between the two CF<sub>3</sub> resonances at slow regime exchange. In the case of an equal population of the two helices (i.e. h.e. = 0%), the  $\delta_{\text{obs}}$  value corresponds to the  $\delta_{\text{mean}}$  value. It is therefore possible to estimate the sign of the screw-sense by determining the relative position of the  $\delta_{\text{obs}}$  value with respects to the  $\delta_{\text{mean}}$  chemical shift. For instance, the fluorinated peptide **4-(S)** displays at room temperature (293 K) a single CF<sub>3</sub> resonance at  $\delta_{\text{obs}} = -75.7$  ppm and, two CF<sub>3</sub> resonances ( $-75.3$  ppm and  $-78.0$  ppm) at slow exchange regime, from which  $\Delta\delta_{\text{slow}} = 2.7$  ppm and  $\delta_{\text{mean}} = -76.65$  ppm have been deduced (Figure 6B). The helical excess (h.e.) value of peptide **4-(S)** was found to be +70%, in good agreement with the helical excess assessed using low temperature <sup>19</sup>F NMR (Table 3). The peptide **4-(R)** exhibits similar helical excess with opposite sign (–70%). The peptides **3-(S)** and **3-(R)** show helical excess values of +90% and –94%, respectively, slightly higher than those obtained using low temperature <sup>19</sup>F NMR (ca. 12% increase).

The chemical shift values of the two CF<sub>3</sub> resonances at slow regime exchange, and consequently the  $\Delta\delta_{\text{slow}}$  and the  $\delta_{\text{mean}}$  values, were found to be similar within the Cbz- and Ac-protected series, respectively. Therefore, the quantification and the assignment of the screw-sense preference of related fluorinated Aib oligomers of peptides **3** and **4** could be easily deduced by extrapolating directly from the chemical shift value of the coalesced <sup>19</sup>F NMR signal observed at room temperature ( $\delta_{\text{obs}}$ ). Finally, we estimated the energy barrier of the 3<sub>10</sub>-helix interconversion of the fluorinated Aib oligomers by dynamic NMR study. The coalescence temperatures ( $T_c$ ) of peptides **3** and **4** were found to be similar ( $T_c \approx 243$  K) corresponding to an energy barrier of  $\Delta G^\ddagger \approx 11.1$  kcal.mol<sup>–1</sup> (See Supporting Information Table S10). This value is in good agreement with the one reported for Aib foldamer ( $\Delta G^\ddagger \approx 11$  kcal.mol<sup>–1</sup> at 265 K).<sup>[59,60]</sup>

## Conclusion

We have reported the synthesis of Aib-based short fluorinated foldamers containing α-Tfm-Ala as a chiral controller of the helical screw-sense at the N-terminal position. NMR studies and X-ray crystallography confirmed the presence of 3<sub>10</sub> helix type and CD spectroscopy indicated a right-handed screw-sense preference for the (S)-TfmAla enantiomers and left-handed screw-sense

preference for the (R)-TfmAla form. The selectivity of the screw-sense is reversed compared to that induced by the non-fluorinated L-α-MeVal chiral inducer due to the electronic properties of the CF<sub>3</sub> group. This <sup>19</sup>F NMR probe allows the easy determination of both the magnitude of the screw-sense preference and the assignment of its sign. Moreover, the energy barrier of the 3<sub>10</sub> helix interconversion has been determined using <sup>19</sup>F NMR. This work demonstrates that <sup>19</sup>F NMR is an easy to handle tool to provide valuable insights into the structuration and the kinetic and thermodynamic parameters of fluorinated foldamers. As this technique avoids the problem of overlapping NMR signals inherent to <sup>1</sup>H NMR, we may now consider using this probe to further study the behavior of fluorinated foldamers in interaction with various biological partners such as proteins and membrane models.

## Experimental Section

Deposition Numbers [2107837](#) (for **4-(S)**) contain the supplementary crystallographic data for this paper. These data are provided free of charge by the joint Cambridge Crystallographic Data Centre and Fachinformationszentrum Karlsruhe [Access Structures service](#).

## Acknowledgements

The CY Initiative of Excellence (grant "Investissements d'Avenir" INEX 2019 FluoSPep) is thanked for financial support of Lizeth Boderio. Authors thank Dr. Pascal Retailleau (Departement of X-ray crystallography at Institut de Chimie des Substances Naturelles – UPS, CNRS-UPR2301 – Gif sur Yvette) for help with the crystal structure solution.

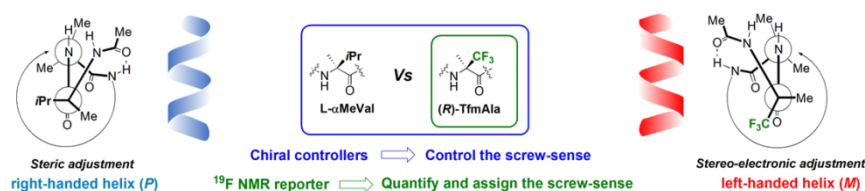
**Keywords:** foldamers • helical structures • fluorinated peptides • circular dichroism • conformational analysis

- [1] S. H. Gellman, *Acc. Chem. Res.* **1998**, 31, 173–180.
- [2] C. M. Goodman, S. Choi, S. Shandler, W. F. DeGrado, *Nat. Chem. Biol.* **2007**, 3, 252–262.
- [3] R. Gopalakrishnan, A. I. Frolov, L. Knerr, W.J. Drury, E. Valeur, *J. Med. Chem.* **2016**, 59, 9599–9621.
- [4] I. M. Mándity, F. Fülöp, *Expert Opin. Drug Discov.* **2015**, 10, 1163–1177.
- [5] M. Oba, *ChemBioChem* **2019**, 20, 2041–2045.
- [6] M. Oba, Y. Ito, T. Umeno, T. Kato, M. Tanaka, *ACS Biomater. Sci. Eng.* **2019**, 5, 5660–5668.
- [7] T. Misawa, N. Ohoka, M. Oba, H. Yamashita, M. Tanaka, M. Naito, Y. Demizu, *Chem. Commun.* **2019**, 55, 7792–7795.
- [8] C. Douat, C. Aisenbrey, S. Antunes, M. Decossas, O. Lambert, B. Bechinger, A. Kichler, G. Guichard, *Angew. Chem. Int. Ed.* **2015**, 54, 11133–11137.
- [9] H. Yokoo, T. Misawa, Y. Demizu, *Chem. Rec.* **2020**, 20, 912–921.
- [10] N. P. Chongsirawatana, J. A. Patch, A. M. Czyzewski, M. T. Dohm, A. Ivankin, D. Gidalevitz, R. N. Zuckermann, A. E. Barron, *Proc. Natl. Acad. Sci. U. S. A.* **2008**, 105, 2794–2799.
- [11] S. Das, K. Ben Haj Salah, M. Djibo, N. Inguibert, *Arch. Biochem. Biophys.* **2018**, 658, 16–30.



- [12] M. Hirano, C. Saito, C. Goto, H. Yokoo, R. Kawano, T. Misawa, Y. Demizu, *ChemPlusChem* **2020**, *85*, 2731–2736.
- [13] J. D. Sadowsky, W. D. Fairlie, E. B. Hadley, H. S. Lee, N. Umezawa, Z. Nikolovska-Coleska, S. Wang, D. C. S. Huang, Y. Tomita, S. H. Gellman, *J. Am. Chem. Soc.* **2007**, *129*, 139–154.
- [14] G. L. Montalvo, Y. Zhang, T. M. Young, M. J. Costanzo, K. B. Freeman, J. Wang, D. J. Clements, E. Magavern, R. W. Kavash, R. W. Scott, et al., *ACS Chem. Biol.* **2014**, *9*, 967–975.
- [15] C. Toniolo, M. Crisma, F. Formaggio, C. Peggion, *Biopolym. - Pept. Sci. Sect.* **2001**, *60*, 396–419.
- [16] M. Venanzi, E. Gatto, F. Formaggio, C. Toniolo, *J. Pept. Sci.* **2017**, *23*, 104–116.
- [17] C. Adam, A. D. Peters, M. G. Lizio, G. F. S. Whitehead, V. Diemer, J. A. Cooper, S. L. Cockroft, J. Clayden, S. J. Webb, *Chem. Eur. J.* **2018**, *24*, 2249–2256.
- [18] C. Toniolo, H. Brückner, *Peptaibiotics: Fungal Peptides Containing  $\alpha$ -Dialkyl  $\alpha$ -Amino Acids*. Wiley-VCH, Weinheim, Germany, **2009**.
- [19] J. Solà, M. Helliwell, J. Clayden, *J. Am. Chem. Soc.* **2010**, *132*, 4548–4549.
- [20] M. De Poli, M. De Zotti, J. Raftery, J. A. Aguilar, G. A. Morris, J. Clayden, *J. Org. Chem.* **2013**, *78*, 2248–2255.
- [21] M. De Poli, L. Byrne, R. A. Brown, J. Solà, A. Castellanos, T. Boddaert, R. Wechsler, J. D. Beadle, J. Clayden, *J. Org. Chem.* **2014**, *79*, 4659–4675.
- [22] B. A. F. Le Bailly, J. Clayden, *Chem. Commun.* **2016**, *52*, 4852–4863.
- [23] M. G. Lizio, V. Andrushchenko, S. J. Pike, A. D. Peters, G. F. S. Whitehead, I. J. Victória-Yrezábal, S. T. Mutter, J. Clayden, P. Bouř, E. W. Blanch, S. J. Webb, *Chem. Eur. J.* **2018**, *24*, 9399–9408.
- [24] H. Mei, J. Han, K. D. Klika, K. Izawa, T. Sato, N. A. Meanwell, V. A. Soloshonok, *Eur. J. Med. Chem.* **2020**, *186*, 111826.
- [25] J. Moschner, V. Stulberg, R. Fernandes, S. Huhmann, J. Leppkes, B. Kokscho, *Chem. Rev.* **2019**, *119*, 10718–10801.
- [26] D. Gimenez, J. A. Aguilar, E. H. C. Bromley, S. L. Cobb, *Angew. Chem. Int. Ed.* **2018**, *57*, 10549–10553.
- [27] J. Cho, K. Sawaki, S. Hanashima, Y. Yamaguchi, M. Shiro, K. Saigo, Y. Ishida, *Chem. Commun.* **2014**, *50*, 9855–9857.
- [28] A. Hassoun, C. M. Grison, R. Guillot, T. Boddaert, D. J. Aitken, *New J. Chem.* **2015**, *39*, 3270–3279.
- [29] C. Li, S.-F. Ren, J.-L. Hou, H.-P. Yi, S.-Z. Zhu, X.-K. Jiang, Z.-T. Li, *Angew. Chem. Int. Ed.* **2005**, *44*, 5725–5729.
- [30] C. F. Wu, Z.-M. Li, X.-N. Xu, Z.-X. Zhao, X. Zhao, R.-X. Wang, Z.-T. Li, *Chem. Eur. J.* **2014**, *20*, 1418–1426.
- [31] A. Ueda, M. Ikeda, T. Kasae, M. Doi, Y. Demizu, M. Oba, M. Tanaka, *ChemistrySelect* **2020**, *5*, 10882–10886.
- [32] S. L. Grage, S. Kara, A. Bordessa, V. Doan, F. Rizzolo, M. Putzu, T. Kubař, A. M. Papini, G. Chaume, T. Brigaud, S. Afonin, A. S. Ulrich, *Chem. Eur. J.* **2018**, *24*, 4328–4335.
- [33] D. Maisch, P. Wadhvani, S. Afonin, C. Böttcher, B. Kokscho, A. S. Ulrich, *J. Am. Chem. Soc.* **2009**, *131*, 15596–15597.
- [34] J. R. Robalo, S. Huhmann, B. Kokscho, A. Vila Verde, *Chem* **2017**, *3*, 881–897.
- [35] C. Gadais, E. Devillers, V. Gasparik, E. Chelain, J. Pytkowicz, T. Brigaud, *ChemBioChem* **2018**, *19*, 1026–1030.
- [36] J. R. Robalo, A. Vila Verde, *Phys. Chem. Chem. Phys.* **2019**, *21*, 2029–2038.
- [37] E. N. G. Marsh, *Acc. Chem. Res.* **2014**, *47*, 2878–2886.
- [38] A. A. Berger, J. S. Völler, N. Budisa, B. Kokscho, *Acc. Chem. Res.* **2017**, *50*, 2093–2103.
- [39] P. Shah, A. D. Westwell, *J. Enzyme Inhib. Med. Chem.* **2007**, *22*, 527–540.
- [40] S. Huhmann, B. Kokscho, *Eur. J. Org. Chem.* **2018**, 3667–3679.
- [41] N. A. Meanwell, *J. Med. Chem.* **2018**, *61*, 5822–5880.
- [42] D. Gimenez, A. Phelan, C. D. Murphy, S. L. Cobb, *Beilstein J. Org. Chem.* **2021**, *17*, 293–318.
- [43] S. J. Pike, M. De Poli, W. Zawodny, J. Raftery, S. J. Webb, J. Clayden, *Org. Biomol. Chem.* **2013**, *11*, 3168–3176.
- [44] R. A. Brown, T. Marcelli, M. De Poli, J. Solà, J. Clayden, *Angew. Chem. Int. Ed.* **2012**, *51*, 1395–1399.
- [45] J. Solà, S. P. Fletcher, A. Castellanos, J. Clayden, *Angew. Chem. Int. Ed.* **2010**, *49*, 6836–6839.
- [46] J. Clayden, A. Castellanos, J. Solà, G. A. Morris, *Angew. Chem. Int. Ed.* **2009**, *48*, 5962–5965.
- [47] S. J. Pike, J. Raftery, S. J. Webb, J. Clayden, *Org. Biomol. Chem.* **2014**, *12*, 4124–4131.
- [48] E. Devillers, J. Pytkowicz, E. Chelain, T. Brigaud, *Amino Acids* **2016**, *48*, 1457–1468.
- [49] G. Chaume, N. Lensen, C. Caupène, T. Brigaud, *Eur. J. Org. Chem.* **2009**, 5717–5724.
- [50] C. Toniolo, A. Polese, F. Formaggio, M. Crisma, J. Kamphuis, *J. Am. Chem. Soc.* **1996**, *118*, 2744–2745.
- [51] F. Leroux, *ChemBioChem* **2004**, *5*, 644–649.
- [52] T. Boddaert, J. Solà, M. Helliwell, J. Clayden, *Chem. Commun.* **2012**, *48*, 3397–3399.
- [53] C. Toniolo, E. Benedetti, *Trends Biochem. Sci.* **1991**, *16*, 350–353.
- [54] T. Cierpicki, J. Otlewski, *J. Biomol. NMR* **2001**, *21*, 249–261.
- [55] R. Gratias, R. Konat, H. Kessler, M. Crisma, G. Valle, A. Polese, F. Formaggio, C. Toniolo, Q. B. Broxterman, J. Kamphuis, *J. Am. Chem. Soc.* **1998**, *120*, 4763–4370.
- [56] G. Wagner, D. Neuhaus, E. Wörgötter, M. Vařák, J. H. R. Kägi, K. Wüthrich, *J. Mol. Biol.* **1986**, *187*, 131–135.
- [57] G. Jung, H. Brückner, R. Bosch, W. Winter, H. Schaal, J. Strähle, *Liebigs Ann. Chem.* **1983**, 1096–1106.
- [58] J. Solà, G. A. Morris, J. Clayden, *J. Am. Chem. Soc.* **2011**, *133*, 3712–3715.
- [59] R.-P. Hummel, C. Toniolo, G. Jung, *Angew. Chem. Int. Ed. Engl.* **1987**, *26*, 1150–1152.
- [60] M. Kubasik, J. Kotz, C. Szabo, T. Furlong, J. Stace, *Biopolymers* **2005**, *78*, 87–95.
- [61] M. De Zotti, B. Biondy, M. Crisma, C. U. Hjørringgaard, A. Berg, H. Brückner, C. Toniolo, *Biopolymers* **2012**, *98*, 36–49.
- [62] M. Tomsett, I. Maffucci, B. A. F. Le Bailly, L. Byrne, S. M. Bijvoets, M. G. Lizio, J. Raftery, C. P. Butts, S. J. Webb, A. Continib, J. Clayden, *Chem. Sci.* **2017**, *8*, 3007–3018.
- [63] B. A. F. Le Bailly, L. Byrne, J. Clayden, *Angew. Chem. Int. Ed. Engl.* **2016**, *55*, 2132–2136.
- [64] L. Byrne, J. Solà, T. Boddaert, T. Marcelli, R. W. Adams, G. A. Morris, J. Clayden, *Angew. Chem. Int. Ed.* **2014**, *53*, 151–155.
- [65] D. Leibfritz, R. M. Brunne, T. Weihrauch, J. Steltena, E. T. K. Haupt, W.-D. Stohrer, *Liebigs Ann. Chem.* **1989**, 1017–1027.

## Entry for the Table of Contents



The chiral  $\alpha$ -trifluoromethylalanine is shown to induce and control the screw-sense preference of short Aib oligomers. Due to the electronic properties of the  $\text{CF}_3$  group, the screw-sense is inversed compared to that induced by its non-fluorinated isosteric L- $\alpha$ -MeVal analogue. It also plays the role of  $^{19}\text{F}$  NMR reporter allowing the easy determination of both the magnitude of the screw-sense preference and the assignment of its sign.

Institute and/or researcher Twitter usernames: @BioCIS